Article

Global Proteomics Analysis of Circulating Extracellular Vesicles Isolated from Lung Transplant Recipients

Sandhya Bansal, Marissa McGilvrey, Krystine Garcia-Mansfield, Ritin Sharma, Ross M. Bremner, Michael A. Smith, Ramsey Hachem, Patrick Pirrotte, and Thalachallour Mohanakumar*

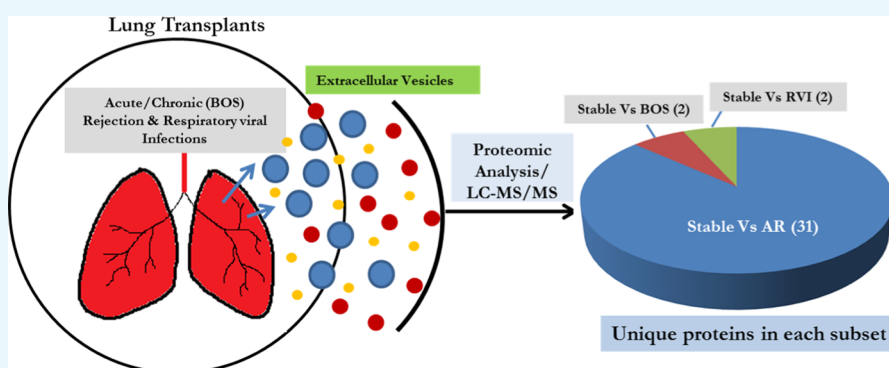Cite This: *ACS Omega* 2020, 5, 14360−14369

Read Online

ACCESS | Metrics & More | Article Recommendations | Supporting Information

ABSTRACT: Lung transplant recipients (LTxRs) with acute rejection (AR) and chronic rejection (bronchiolitis obliterans syndrome [BOS]) induce circulating exosomes known to contain donor human leukocyte antigens and lung-associated self-antigens. Here, we sought to identify proteomic signatures in circulating extracellular vesicles (EVs) that differentiate LTxRs in 4 groups: stable, AR, BOS, or respiratory viral infection (RVI). EVs were isolated from plasma from patients in each group via ultracentrifugation. EV protein cargoes were prepared for shotgun proteomics using liquid chromatography−tandem mass spectrometry. We identified 2 unique proteins for AR, 4 for RVI, 24 for BOS, and 8 for stable LTxRs. Differential analysis of AR, BOS, RVI, and stable proteins identified significantly deregulated proteins ($p < 0.05$, $\log_2(\text{fold change}) > \pm 1$) in each condition (31, 2, and 2, respectively). EVs from LTxRs with AR contained proteins involved in immunoglobulin, complement regulation, coagulation, and innate and adaptive immune response pathways. EVs from LTxRs with BOS revealed enriched immunoglobulin receptors and a carboxypeptidase N catalytic chain. EVs from LTxRs with RVI had an enriched macrophage-stimulating factor. We found unique signatures in LTxRs with AR, BOS, and RVI, highlighting complex immune mechanisms underlying lung allograft rejection. Proteomic signatures in LTxRs' circulating EVs provided insights into immunological mechanisms of graft rejection and RVI.

1. INTRODUCTION

Lung transplantation (LTx) is a treatment option for patients with end-stage respiratory disease such as idiopathic pulmonary fibrosis, chronic obstructive pulmonary disease, cystic fibrosis, and other interstitial lung disease.[1] Despite immunosuppressive measures, post-LTx recovery can be challenged by acute rejection (AR) or chronic rejection. The median survival after LTx is just 5.8 years, and this is the shortest survival compared with all other solid organ transplants, results primarily from chronic rejection.[2] Several risk factors for AR or chronic rejection have been proposed, including immune responses to human leukocyte antigen (HLA), development of donor-specific antibody (DSA) against HLA, immune response to lung-associated self-antigens (SAgs), and respiratory viral infection (RVI).[3−5] The contribution and interplay of factors underlying each of these

mechanisms in modulating the immune responses of LTx recipients (LTxRs) has not been fully characterized.[6]

Extracellular vesicles (EVs) play an important role in defining the immunopathogenesis of lung disease.[7] EVs are a family of particles released by cells, and they are involved in various physiological functions. EVs vary in size, morphology, and content and are classified based on the mechanism of their release. Exosomes, which are membrane-bound EVs, result from the fusion of late endosomes with the plasma membrane

(<200 nm in diameter), whereas microvesicles and apoptotic bodies (typically 200−1000 nm in diameter) are the result of vertical trafficking of molecules to the plasma membrane, where molecules are shed in the form of EVs into the extracellular space. Several reports demonstrated that EVs carry a diverse cargo of proteins, lipids, metabolites, and RNAs (mRNAs and noncoding RNAs, including microRNAs).[8] EVs have also been shown to contribute to intercellular communication, with critical roles in cancer, the spread of infection, and physiological processes such as stress, inflammation, wound healing, coagulation, and angiogenesis.[9] We recently reported that circulating exosomes isolated from LTxRs with AR or bronchiolitis obliterans syndrome (BOS) contain DSA, lung SAgs, major histocompatibility complex class II molecules, costimulatory molecules CD80 and CD86, transcription factor NF-kB, CIITA, and 20S proteasome.[10] However, the biological functions and fate of EVs released after LTx remain unknown. The goal of this study is to identify, compare, and contrast proteomic signatures in the circulating EVs isolated from LTxRs diagnosed with AR, RVI, or BOS vs stable LTxRs, using mass spectrometry to clarify the molecular mechanisms underlying lung allograft rejection.

2. RESULTS AND DISCUSSION

2.1. EV Protein Cargo Characterization in LTxRs. Proteomic analysis of circulating EVs identified a total of 2834 peptides mapping to 236 nonredundant proteins. Overall, 136 proteins (57.6%) were common to all conditions (Figure 1)
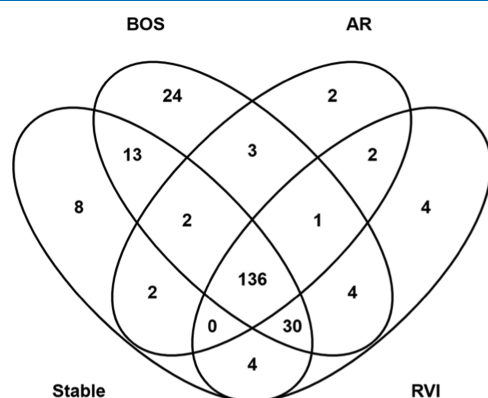

Figure 1. Venn diagram of proteins identified in extracellular vesicles isolated from patients in 4 conditions after lung transplant. Abbreviations: AR, acute rejection; BOS, bronchiolitis obliterans syndrome; and RVI, respiratory viral infection.

and 8, 24, 2, and 4 proteins were unique to LTxRs in the stable, BOS, AR, and RVI groups, respectively. An average of 164 proteins was identified in BOS (n = 3) with an average of 78% mapping to ExoCarta. In patients with AR (n = 3), an average of 128 proteins was identified and 79% were present in ExoCarta. An average of 145 proteins was identified in RVI (n = 3) and 76% were in ExoCarta. For stable patients (n = 5), an average of 143 proteins was identified with 79% annotated in ExoCarta. (Table 1). Eight proteins uniquely identified in EVs from stable LTxRs (ACTR2, EFEMP1, IGKV1−16, IGKV1D-39, IGLV2−23, GNL1, PFKP, and S100-A12; Figure 1 and Table 2) are involved in the transport of small molecules, signal transduction, hemostasis, and extracellular matrix organization. Two proteins uniquely identified in AR

Table 1. Total Protein Identifications in EVs from Patients Post LTx[a]

group	total peptides	total proteins	proteins mapped to ExoCarta (%)
BOS	2793	138	114 (83)
	3245	190	145 (76)
	3211	163	124 (76)
AR	2373	122	99 (81)
	2636	137	103 (75)
	2451	125	100 (80)
RVI	3190	161	126 (78)
	2828	137	103 (75)
	2867	137	103 (75)
stable	2547	135	108 (80)
	3136	166	125 (75)
	2788	142	102 (72)
	2790	137	117 (85)
	2824	135	108 (80)

[a]Abbreviations: EVs, extracellular vesicles; LTx, lung transplant; BOS, bronchiolitis obliterans syndrome; AR, acute rejection; RVI, respiratory viral infection.

(CFHR2 and IGKV1−33; Figure 1 and Table 2) are associated with immunoglobulin and complement regulation.

The 24 proteins uniquely identified in LTxRs with BOS (ATP2A3, CANX, CD36, CPB2, ENDOD1, F9, GANAB, GP1BB, HIST1H4A, HSPA5, IGHV1−3, IGKV3D-20, IGLV4−60, ITGA6, ITGB1, MYH9, MYL6, PDIA3, PF4, PSMA2, PSMA7, PTGS1, TTYH3, and YWHAZ; Figure 1 and Table 2) are associated with immune activation, including immunoglobulin synthesis, programmed cell death, and DNA repair. EVs from LTxRs with RVI harbored 4 unique proteins (GPX3, HSPG2, IGHD, and IGLV9−49; Figure 1 and Table 2) linked to macrophage and immune activation.

2.2. Differential Analysis of EV Proteomes from LTxR Subgroups. Differential analysis across stable LTxRs and those with BOS, AR, and RVI revealed significantly (p < 0.05, log2 fold change (FC) > ±1) upregulated or downregulated proteins listed in Table 3 and visualized on the volcano plots (Figure 2). BOS showed an increase in the carboxypeptidase N catalytic chain (CPN1, p = 0.01) and a decrease in the polymeric immunoglobulin receptor (PIGR, p = 0.02), while AR showed an increase in several complement proteins including C3 (p = 0.006), C6 (p = 0.0009), C7 (p = 0.01), CFI (p = 0.005), CFB (p = 0.03), CFH (p = 0.03), and C8B (p = 0.04) and a decrease in immunoglobulin-associated proteins (IGLV2-18 (p = 0.01), IGLV7-46 (p = 0.01), and IGKV6D-21 (p = 0.04)). EVs from LTxRs with RVI identified two differentially abundant proteins: macrophage-stimulating protein (MST1) (increased, p = 0.01) and IGCL7 (immunoglobulin lambda constant 7) (decreased, p = 0.04).

Unsupervised clustering (Supporting Information, Figure S1) of the 35 significant differentially abundant proteins showed that the AR patients have a very distinct abundance profile of these proteins compared to the other LTxR conditions while a wide heterogeneity persists between other LTxR conditions. Details on proteins used for each pairwise analysis are provided in Supporting Information, Table S1.

2.3. LTxR-Derived EVs Contain Distinct Functional Signatures. Gene set enrichment analysis (GSEA) identified pathways and biological processes enriched in stable LTxRs and LTxRs with AR, BOS, or RVI (Figure 3). In LTxRs with AR, upregulated proteins contributed to a positive enrichment

Table 2. Unique Proteins in Each LTx Condition[a]

LTxR group	uniprot accession	gene	description	molecular function	biological role	# of patients
BOS (N = 3)	Q93084-4	ATP2A3	sarcoplasmic/endoplasmic reticulum calcium ATPase 3	translocase	calcium transport	1
	P05556	ITGB1	integrin β-1	receptor	cell adhesion	1
	P16671-4	CD36	platelet glycoprotein 4	receptor	cell adhesion	1
	P23229-7	ITGA6	Integrin α-6	receptor	cell adhesion	1
	P35579	MYH9	myosin-9	actin binding	cell adhesion	1
	P02776	PF4	platelet factor 4	cytokine	chemotaxis	1
	O14818	PSMA7	proteasome subunit α type-7	hydrolase	component of the 20S core proteasome complex	1
	P25787	PSMA2	proteasome subunit α type-2	hydrolase	component of the 20S core proteasome complex	1
	P62805	H4C1	histone H4	DNA binding	core component of nucleosome	1
	Q14697	GANAB	neutral α-glucosidase AB	hydrolase	glycan metabolism	1
	P00740-2	F9	coagulation factor IX	hydrolase	hemostasis	1
	P13224	GP1BB	platelet glycoprotein Ib β chain	protein binding	hemostasis	1
	Q96IY4	CPB2	carboxypeptidase B2	hydrolase	hemostasis	1
	A0A075B6I1	IGLV4−60	immunoglobulin lambda variable 4−60	antigen binding	immunity	1
	A0A0C4DH25	IGKV3D-20	immunoglobulin kappa variable 3D-20	antigen binding	immunity	1
	A0A0C4DH29	IGHV1−3	immunoglobulin heavy variable 1−3	antigen binding	immunity	1
	Q9C0H2-3	TTYH3	protein tweety homolog 3	ion channel	ion transport	1
	P23219-4	PTGS1	prostaglandin G/H synthase 1	dioxygenase	lipid metabolism	1
	O94919	ENDOD1	endonuclease domain-containing 1 protein	endonuclease activity	platelet degranulation	1
	P30101	PDIA3	protein disulfide-isomerase A3	isomerase	protein folding	1
	P11021	HSPA5	endoplasmic reticulum chaperone BiP	chaperone	protein folding and quality control	1
	P27824-3	CANX	calnexin	chaperone	protein folding and quality control	1
	P60660-2	MYL6	myosin light polypeptide 6	motor protein	regulatory light chain of myosin	1
	P63104	YWHAZ	14-3-3 protein zeta/delta	adapter protein	signal transduction	1
AR (N = 3)	P01594	IGKV1−33	immunoglobulin kappa variable 1−33	antigen binding	immunity	1
	P36980-2	CFHR2	complement factor H-related protein 2	protein binding	regulation of complement activation	1
RVI (N = 3)	A0A0B4J1Y8	IGLV9−49	immunoglobulin lambda variable 9-49	antigen binding	immunity	1
	P01880	IGHD	immunoglobulin heavy constant delta	antigen binding	immunity	1
	P22352	GPX3	glutathione peroxidase 3	oxidoreductase	cellular response to oxidative stress	2
	P98160	HSPG2	basement membrane-specific heparan sulfate proteoglycan core protein	amyloid-β binding	angiogenesis	1
stable (N = 5)	P04432	IGKV1D-39	immunoglobulin kappa variable 1D-39	antigen binding	immunity	2
	P01705	IGLV2−23	immunoglobulin lambda variable 2−23	antigen binding	immunity	1
	P04430	IGKV1−16	immunoglobulin kappa variable 1−16	antigen binding	Immunity	1
	P80511	S100-A12	Protein S100-A12	metal binding	immunity	1
	Q01813-2	PFKP	ATP-dependent 6-phosphofructokinase, platelet type	ATP binding	glycolysis	1
	P61160	ACTR2	actin-related protein 2	actin binding	constituent of ARP2/3 complex	1
	P36915-2	GNL1	guanine nucleotide-binding protein-like 1	GTPase activity	signal transduction	1
	Q12805-5	EFEMP1	EGF-containing fibulin-like extracellular matrix protein 1	EGF and EGFR binding	signal transduction	1

[a]Proteins present in 3 out of 3 technical replicates for each patient were compared. Proteins unique to a LTx group are presented, with the number of patients each protein was identified in. Functional information is taken from protein annotation in the Uniprot database.

of 4 gene sets (hallmark coagulation, innate immune system, regulation of intracellular transduction, and activation of immune response). Downregulated proteins were associated with a negatively enriched functional gene set (small molecule metabolic process; Figure 3A).

Fifteen gene sets were significantly enriched in LTxRs with BOS (Figure 3B). Twelve sets were negatively enriched in LTxRs with BOS; of these, 2 gene sets are associated with cellular death. The top 3 negatively enriched sets are associated

with catabolic processes. Of the 3 positively enriched sets, 2 are associated with regulation of the extracellular matrix (matrisome-associated and extracellular matrix regulators) and the third is associated with complement system response (lectin pathway).

In LTxRs with RVI, GSEA identified 10 positively and 2 negatively enriched gene sets, associated with upregulated and downregulated proteins, respectively (Figure 3C). Four of the positively enriched sets are associated with lipid metabolism

Table 3. Significant Differentially Abundant Proteins in EVs of LTxRs: Significant Differentially Abundant Proteins ($p <$ 0.05 and $\log_2(FC) > \pm 1$) in Each Rejection Condition Compared to Stable[a]

gene names	p-value	p-Adj (BH)	log₂(FC)
LTxRs with AR vs stable LTxRs			
C6	0.001	0.0834	1.312
AMBP	0.0025	0.055	1.295
FBLN1	0.0026	0.0767	1.169
ITIH4	0.003	0.1732	1.795
CFI	0.0054	0.0973	1.745
C3	0.0064	0.0808	1.443
APOC3	0.0077	0.0934	1.799
VWF	0.0103	0.1732	1.395
C7	0.0115	0.0371	1.492
CFB	0.0364	0.0543	1.055
CFH	0.0382	0.0543	1.116
ECM1	0.0419	0.1732	1.522
F11	0.0431	0.1732	1.372
ITIH1	0.044	0.1732	1.104
C8B	0.0477	0.1732	1.109
CLU	0.0001	0.1732	−1.247
VTN	0.0011	0.134	−1.451
GAPDH	0.0012	0.1732	−3.914
PON1	0.0036	0.0178	−1.805
KLKB1	0.0079	0.0834	−1.313
IGLV2-18	0.0179	0.1732	−2.568
IGLV7-46	0.0181	0.1732	−1.8
APOA1	0.02	0.0371	−1.162
IGLC7	0.0295	0.1279	−1.201
VTN	0.0303	0.0578	−3.215
IGLV1-40	0.0322	0.1732	−1.114
APOA2	0.035	0.1732	−1.412
IGHM	0.0353	0.1279	−1.421
ACTB	0.0361	0.1732	−2.068
IGKV6D-21	0.0445	0.1732	−2.414
TLN1	0.0477	0.0371	−3.413
LTxRs with BOS vs Stable LTxRs			
CPN1	0.0141	0.945	1.134
PIGR	0.0243	0.945	−1.403
LTxRs with RVI vs Stable LTxRs			
MST1	0.0109	0.865	1.363
IGLC7	0.0407	0.865	−1.324

[a]Abbreviations: EVs, extracellular vesicles; LTx, lung transplant; LTxRs, lung transplant recipients, AR, acute rejection; BOS, bronchiolitis obliterans syndrome; RVI, respiratory viral infection.

(regulation of the lipid metabolic process, cellular lipid metabolic process, lipid metabolic process, and regulation of lipid localization). The 2 negatively enriched sets are associated with immune response (innate immune system and defense response to bacterium).

Across the 3 GSEA analyses, only two enriched gene sets were shared between LTxRs with rejection; the innate immune system is positively enriched in the setting of AR and is negatively enriched in LTxRs with RVI. Negative regulation of cellular component organization is negatively enriched in LTxRs with BOS and is positively enriched in LTxRs with RVI.

2.4. Validation of Key Proteins in Each Clinical Condition Using Immunoblot. To validate our findings by Western blot, we selected several differentially abundant proteins (C3 for AR, CPN1 for BOS, and MST1 for RVI). C3

was present in EVs from AR samples, which are ∼2.3-fold higher as compared to EVs from stable samples (Figure 4a,d). CPN1 was present in 4.0-fold higher quantities in EVs from BOS than stable (Figure 4b,e). MST1 was 7.0-fold increased in RVI compared to stable patients (Figure 4c,f). Differential abundance of MST1 in RVI, C3 in AR samples, and CPN1 in BOS was statistically significant ($p \leq 0.005$) compared to stable. However, we have done Western blots of MV isolated from normal and did not detect any of the key proteins what we identified post LTx (collagen V and Kα_1 tubulin).

We previously published our observation of increased levels of donor HLA, lung SAgs, transcription factor NF-Kβ, CIITA, and 20S proteasome in circulating exosomes of LTxRs with AR and BOS.[10,11] In the current study, we demonstrated that circulating EVs from LTxRs with AR contained significantly increased levels of immunoglobulin and complement regulatory proteins, along with coagulation factors and plasminogen, compared to stable LTxRs. A report by Naesens et al.[12] showed that renal transplant biopsies classified as cellular rejection contain B lymphocytes capable of producing antibodies (Abs) against donor antigens, along with C3, CD20, and peritubular deposition of C4D. In agreement, our results also showed humoral-pathway activation in LTxRs diagnosed with cellular AR. We demonstrated the upregulation of proteins associated with complement, immunoglobulins, coagulation, and inflammation in LTxRs with cellular rejection. Complement activation is known to have a strong correlation with tissue injury and antibody-mediated rejection,[13] and our results suggest that complement-mediated tissue injury can occur even in patients diagnosed with cellular rejection. Furthermore, our result raises the possibility that complement proteins in circulating EVs can be markers to differentiate cellular rejection with a mixed phenotype (i.e., cellular and humoral) from only having a cellular phenotype.

Extracellular vesicles isolated from LTxRs with BOS showed increased amounts of CPN1, a zinc metalloprotease with a known protective function against vasoactive and inflammatory peptides.[14] CPN levels are associated with complement activation; therefore, higher levels of CPN1 in LTxRs with BOS indicate increased complement activation. EVs from LTxRs with BOS also showed altered levels of PIGR. PIGR binds and transports polymeric immunoglobulin A and immunoglobulin M across the epithelial barrier to mucosal surfaces.[15] Studies have shown that gastroesophageal reflux increases the risk of BOS after LTx.[16] We therefore propose that PIGR may be a contributing factor for gastroesophageal reflux disease (GERD), increasing the risk of BOS.

Extracellular vesicles isolated from LTxRs with symptomatic RVI (e.g., respiratory syncytial virus, coronavirus, rhinovirus, and influenza virus) showed significantly increased levels of MST1, a macrophage-stimulating protein also known as hepatocyte growth factor-like protein, compared to stable LTxRs.[17] MST1/2 is a mediator of innate immune response[18] against viruses, eliciting macrophage phagocytosis as well as cytokines and production of reactive oxygen species. Upregulation of MST1 in EVs isolated from LTxRs with RVI suggests that circulating EVs can be involved in the activation of innate immune responses, which leads to increased cytokine and reactive oxygen species production toward controlling the infection. MST1 is also likely to play an important role in lung tissue regeneration after RVI, as suggested by Narasaraju et al.[19] Thus, our finding of increased levels of MST1 in EVs from LTxRs with RVI strongly suggests
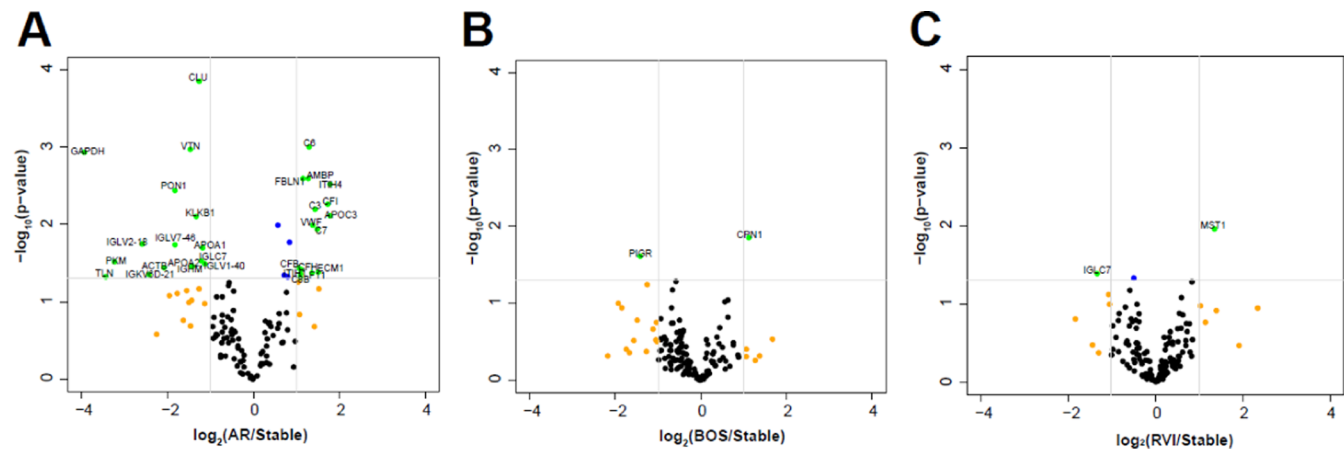
Figure 2. Volcano plots of differentially abundant proteins in LTxRs. $\log_2(\text{FC})$ vs $-\log_{10}(p\text{-value})$ for (A) AR vs stable, (B) BOS vs stable, and (C) RVI vs stable. Green dots ($-\log_{10}(p\text{-value}) > 1.301$ and $\log_2(\text{FC}) > \pm 1$). Orange dots ($\log_2(\text{FC}) > \pm 1$). Blue ($-\log_{10}(p\text{-value}) > 1.301$). Abbreviations: AR, acute rejection; BOS, bronchiolitis obliterans syndrome; and RVI, respiratory viral infection.
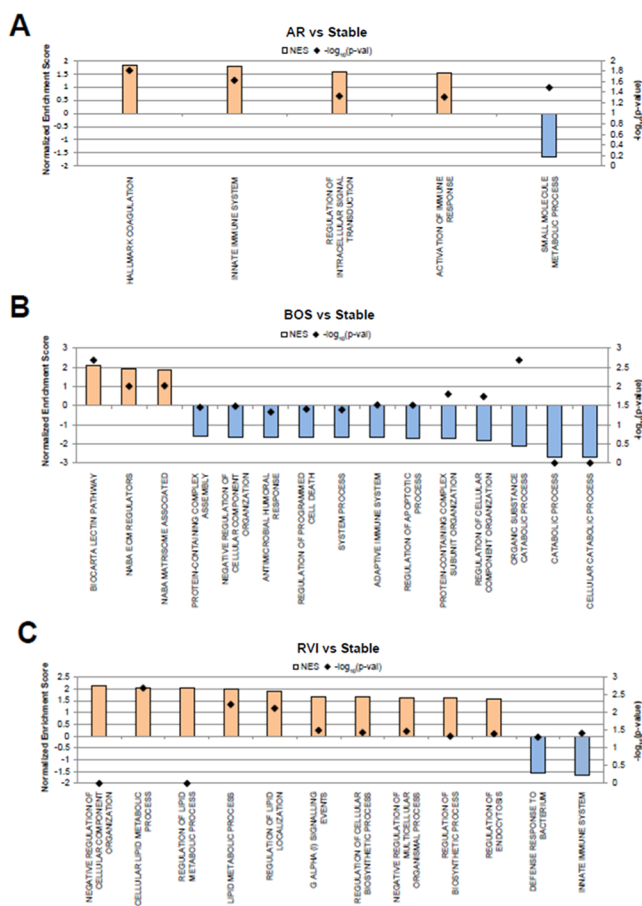

Figure 3. Significantly enriched GSEA-enriched (p-value <0.05) terms from gene ontology biological processes (GOBP) associated with the 3 described conditions vs stable LTxRs. (A) AR vs stable, (B) BOS vs stable, and (C) RVI vs stable. Abbreviations: AR, acute rejection; BOS, bronchiolitis obliterans syndrome; and RVI, respiratory viral infection. The computed normalized enrichment score shows GOBP terms that are increased (orange) or decreased (blue).

that this protein may be involved in the repair of damaged lung epithelium caused by a viral infection. Furthermore, we propose that in LTxRs, MST1 contained in EVs can be used as a protein signature specific to RVI and could be a useful

marker for the challenging differential diagnosis of RVI from acute cellular rejection.

We are identifying proteins in the EV, which are diagnostic for AR, BOS, and RVI. However, these samples were obtained at the time of diagnosis. Further studies are needed to determine the value of these proteins in the EV as a noninvasive biomarker, which will require testing serial samples from a larger cohort. Further, chronic rejection following human LTx is now termed as chronic lung allograft dysfunction, which consists of restrictive allograft syndrome (RAS) and BOS. During this study, we have analyzed only BOS but not RAS and therefore further analysis of EV from RAS needs to be carried out to determine the potential value of unique proteins that may be present in RAS, which may provide further clues to the pathogenesis of RAS vs BOS.

The low number of LTxR specimens from which EVs were characterized is a limitation of this study. This is particularly true for LTxRs with AR, as our data suggest a mixed cellular and humoral phenotype for the LTxRs with AR analyzed thus far. Therefore, follow-up studies should include additional LTxRs diagnosed either with cellular rejection or antibody-mediated rejection. Another shortcoming of this study is that we analyzed only rhinovirus, coronavirus, and metapneumo-virus. Inclusion of LTxRs with other common infections associated with increased risk for BOS (e.g., respiratory syncytial virus and cytomegalovirus) should be considered in future analysis. According to guidelines from the International Society for Heart and Lung Transplantation, chronic lung allograft dysfunction is classified as BOS or RAS, and our analysis has been restricted only to BOS.[24]

3. CONCLUSIONS

The presence of unique proteins and their association with pathways in the EVs isolated from plasma samples of LTxRs with AR, BOS, and RVI provide important mechanistic information about rejection after LTx. In summary, proteomic findings from this study clearly demonstrate not only novel mechanisms for rejection but also the potential of EV protein cargo to distinguish different forms of AR (cellular vs humoral vs mixed). Our results highlight the role of immunoglobulins and complement proteins in BOS, which emphasizes the importance of Abs in the pathogenesis of BOS. The abundance
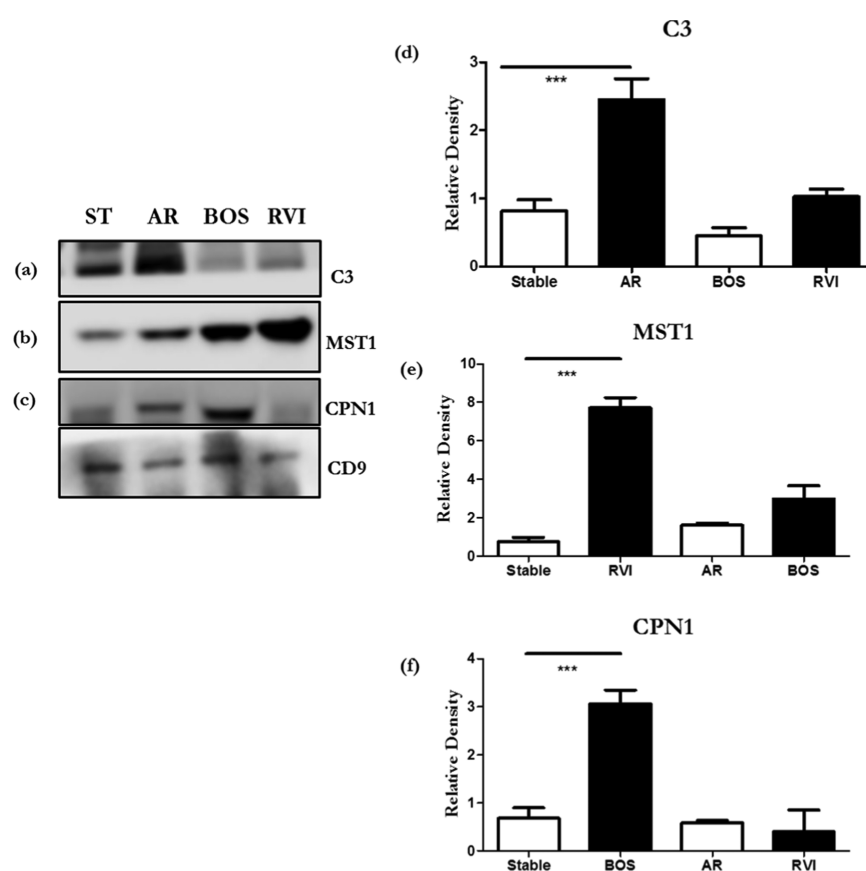
Figure 4. Western blots of significantly differential proteins (a) C3, (b) MST1, and (c) CPN1 in stable, AR, BOS, and RVI samples from exosomes from LTxRs. Densitometry of Western blots (d) C3, (e) MST1, and (f) CPN1. CD9 was used as an internal control for exosomes. The presented data are representative of at least 3 independent experiments. The C3, CPN1, and MST1 levels were normalized to CD9 levels and are shown as relative levels. Data are shown as mean $\pm$ standard deviation (SD). p-values were calculated using a two-tailed unpaired Student's t-test. (***$p <$ 0.005). Abbreviation: ST, stable; AR, acute rejection; BOS, bronchiolitis obliterans syndrome; and RVI, respiratory viral infection.

of MST1 in EVs from LTxRs with RVI suggests that MST1 can be a potential marker to differentiate RVI from AR.

The presence of immunoglobulin and complement proteins in circulating EVs isolated from LTxRs with cellular AR provides a means to differentiate cellular rejection from mixed (i.e., cellular and humoral) rejection. The presence of immunoglobulins in EVs from LTxRs with BOS suggests an important role for Abs, both against DSA and lung-associated SAgs, in the pathogenesis of BOS, as several studies have demonstrated that development of DSA and Abs to lung SAgs is an important risk factor for BOS after LTx.[20−23] In addition, validation using Western blots of several proteins (C3, CPN1, and MST1), which are differentially present in LTxRs with AR, BOS, and RVI, suggests that differentiating between acute/chronic rejection and viral infection after LTx is possible using this subset of protein markers.

4. MATERIALS AND METHODS

4.1. Patient Population. Lung transplant recipients at St. Joseph's Hospital and Medical Center in Phoenix, Arizona, and from Washington University Medical School in St. Louis, Missouri, were selected based on clinical diagnosis of AR, RVI (rhinovirus, metapneumovirus, and coronavirus), BOS, and stable per criterion established by ISHLT.[24] This study was approved by the Institutional Review Boards of St. Joseph's Hospital and Medical Center (IRB #PHXB16-0027-10-18),

and patient samples were collected after informed consent was obtained.

4.2. Sample Collection. Blood samples were collected from patients in acid citrate dextrose solution, and plasma was isolated within 24 h of collection and stored at −80 °C. LTxR demographics are summarized in Table 4.

4.3. EV Enrichment. Extracellular vesicles were isolated from 500 μL of plasma by ultracentrifugation, as previously described.[25] Briefly, the samples were centrifuged at 2000 rcf (20 min, 4 °C) followed by 2 cycles of centrifugation at 10 000 rcf (40 min, 4 °C). The supernatant was diluted with 0.5 mL of phosphate-buffered saline (PBS) and spun for 100 000 rcf (120 min, 4 °C). EV pellets were resuspended in PBS. This final centrifugation step was repeated, and the EV pellets were recovered and stored at −80 °C. EV size distribution was determined using NanoSight (Malvern Panalytical, Malvern, United Kingdom; Figure 5), and EVs used in this report ranged in size from 50 to 200 nm.[26]

4.4. Chemicals and Reagents. The chemicals and solvents used were procured from Sigma-Aldrich (St. Louis, MO) or Thermo Fisher Scientific (Waltham, MA). All chemicals were analytical reagent grade. Formic acid and solvents were liquid chromatography−mass spectrometry (LC−MS/MS) grade. Halt protease and phosphatase-inhibitor cocktail (100×) was obtained from Thermo Fisher Scientific (Waltham, MA). Sequencing-grade enzymes were purchased from Promega (Madison, WI).

Table 4. Demographic Characteristics of 14 Lung Transplant Recipients[a]

variable	N (%)	time of sample collection
mean age, years ± SD	50.3 ± 12.2	
male sex	7 (50)	
white race	14 (100)	
bilateral LTx	14 (100)	
post-LTx diagnosis		
BOS	3 (21)	1.5–2.0 years
AR	3 (21)	6 months
RVI	3 (21)	12–36 months
stable	5 (36)	12–36 months
reason for LTx by post-LTx diagnosis		
BOS		
IPF	3/3 (100)	
AR		
COPD	1/3 (33)	
IPF	2 (67)	
RVI		
COPD	2/3 (67)	
IPF	1/3 (33)	
stable		
COPD	3/5 (60)	
IPF	2/5 (20)	

[a]Abbreviations: LTx, lung transplant; BOS, bronchiolitis obliterans syndrome; AR, acute rejection; RVI, respiratory viral infection; IPF, idiopathic pulmonary fibrosis; COPD, chronic obstructive pulmonary disease.
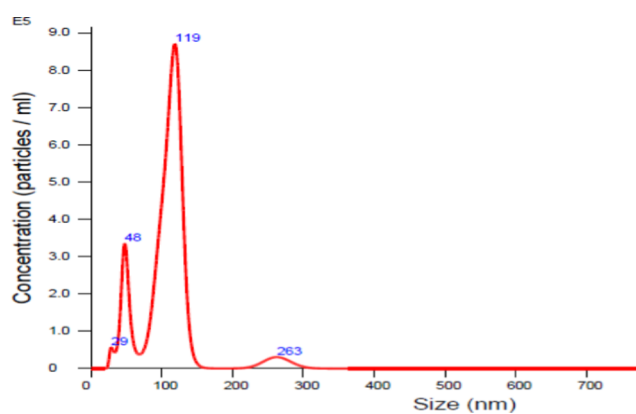
Figure 5. Representative image of size determination of exosomes using NanoSight.

4.5. Protein Extraction and Digestion. Pelleted EVs were thawed and proteins were extracted in 250 μL of 25 mM ammonium bicarbonate buffer (NH_4HCO_3), supplemented with 1% sodium deoxycholate, 1× halt protease, and phosphatase-inhibitor cocktail. Samples were lysed by sonication for 1 min, followed by centrifugation at 21 000 rcf (10 min, 4 °C) to pellet any debris. The supernatant was transferred to 10 kD Amicon Ultrafilters (Sigma-Aldrich, St Louis, MO) to perform filter-aided sample preparation for shotgun proteomic analysis.[27,28] Briefly, extracted proteins were denatured with 8 M urea, reduced in 10 mM dithiothreitol, and alkylated in 50 mM iodoacetamide. Samples were subjected to a buffer exchange in 50 mM NH_4HCO_3, followed by overnight digestion using trypsin at a 1:50 enzyme to protein ratio at 37 °C. Peptides were extracted from the filter at 14 000 rcf, and the flow-through was vacuum-dried and stored at −80 °C until LC−MS/MS analysis was performed.

4.6. LC−MS/MS Analysis. Tryptic peptides were reconstituted in 0.1% formic acid and quantified by the bicinchoninic acid assay for LC−MS/MS analysis on an Orbitrap Fusion Lumos Tribrid (Thermo, Waltham, MA) interfaced with a nanoAcquity UPLC system (Waters, Milford, MA). For each sample acquired in technical triplicates, 800 ng of peptides was first loaded on a trapping column (Acquity UPLC M-Class Trap, two-dimensional (2-D) Symmetry C18, 100 Å pore size, 5 μm particle size, 20 mm length) and washed for 10 min with 99.5% Solvent A (0.1% formic acid in water) and 0.5% solvent B (0.1% formic acid in acetonitrile) at a flow rate of 7.5 μL/min. The trapped peptides were transferred to an analytical column (Acquity UPLC M-Class Peptide BEH C18, 130 Å pore size, 1.7 μm particle size, 100 mm length) and eluted at a flow rate of 500 nL/min using the following gradient: 3−7% B in 1 min, 7−25% B in 25 min, 25−45% B in 10 min, 45−90% B in 0.5 min, 90% B for 1 min, back to initial condition in 0.5 min, and re-equilibration for 10 min. Data-dependent acquisition was performed in Top Speed mode with a duty cycle of 3 s and the following parameters: spray voltage of 1900 V, ion-transfer tube temperature of 275 °C, survey scan in the Orbitrap at a resolution of 120 K at 200 m/z, scan range of 400−1500 m/z, AGC target of 2E5, and maximum ion injection time of 50 ms. Every parent scan was followed by a daughter scan using high-energy collision dissociation of top abundant peaks and detection in the ion trap with following settings: quadrupole isolation mode, isolation window at 1.4 m/z, AGC target of 5E3 with maximum ion injection time of 50 ms, and high-energy collision energy of 35%. Dynamic exclusion was set to 60 s.

4.7. Data Analysis. Mass spectra were matched to the *Homo sapiens* database (2017, SwissProt/UniProtKB) using the Andromeda search engine (MaxQuant v1.6.1.0)[29] with a false discovery rate (FDR) <1%, allowing up to 2 missed cleavages from trypsin. All other MaxQuant settings were set to default. Cysteine carbamidomethylation was set as a fixed modification, and variable modifications of N-terminus acetylation and methionine oxidation were allowed. The peptides were identified using the match between runs feature enabled, and protein intensities were computed using the MaxQuant label-free quantitation (LFQ) algorithm. Iterative rank order normalization (IRON)[30] was used to normalize LFQ intensities across all samples. For each patient, intensities were averaged if the protein was identified in 3 out of 3 technical replicates, otherwise the protein was removed from that patient. Protein intensity was log₂-transformed, and fold change for each protein was calculated between the stable LTxR and each of the three rejection groups. Proteins annotated by MaxQuant as hits to the reverse database (n = 6 proteins), potential contaminants (n = 19 proteins), or without a unique peptide (n = 3 proteins) were not included for differential analysis. Statistical significance of the change in protein abundance between each pairwise analysis (stable LTxR vs each of the three rejection groups) was determined using Student's t-test. A Benjamini−Hochberg test for multiple corrections was also calculated. Proteins with a log₂(fold change) > ±1, corresponding to a 2-fold change from the stable, and a t-test p-value <0.05 were deemed significantly differentially abundant. Proteins were annotated using the ExoCarta reference database.[31] To identify enriched processes and pathways in each rejection condition compared to stable

LTxRs, each protein was ordered by ranking score (RS = $-\log_{10}$ (p-value)* $\pm$ 1, where the directionality matches the fold change) from highest to lowest. Functional enrichment analysis was performed using GSEA against the Gene Ontology Resource (downloaded April 2019).[32]

4.8. Western Blots. Extracellular vesicles isolated with ultracentrifugation[25] were lysed using radioimmunoprecipitation assay buffer containing protease inhibitor cocktails. Protein was estimated using the bicinchoninic acid assay. Western blot was performed to validate the signatures identified by mass spectrometry. Briefly, 30 μg of protein from EVs was resolved via polyacrylamide gel electrophoresis, and the proteins were transferred into a poly(vinylidene difluoride) membrane. The membrane was blocked with 5% nonfat milk in 1× PBS and was probed with Abs to C3 (Abcam, anti-rabbit), CPN1 (Abcam, anti-rabbit), MST1 (Cell Signaling Technology, anti-rabbit), and CD9 (Biolegend, anti-mouse). Secondary Abs conjugated with horseradish peroxidase were used for detection. The blots were washed with PBS-Tween (Thermo Fisher Scientific), developed using the chemiluminescent horseradish peroxidase substrate (Amersham ECL Western Blotting Detection Kit), and exposed using an Odyssey CLx Imaging System (LI-COR Biosciences, Lincoln, NE).

◼ ASSOCIATED CONTENT

Ⓢ Supporting Information

The Supporting Information is available free of charge at https://pubs.acs.org/doi/10.1021/acsomega.0c00859.

> Details of proteins used for each pairwise analysis (Table S1); unsupervised clustering of lung transplant conditions from 35 significant proteins in lung transplant recipients with bronchiolitis obliterans syndrome (BOS), acute rejection (AR), and respiratory viral infection (RVI) compared to stable lung transplant recipients; the AR patients show clearly distinct protein profiles for the 31 differentially abundant proteins compared to the rest of the LTxR groups (Figure S1) (PDF)

◼ AUTHOR INFORMATION

Corresponding Author

Thalachallour Mohanakumar − *Norton Thoracic Institute, St. Joseph's Hospital and Medical Center, Phoenix, Arizona 85013, United States;* ⓞ orcid.org/0000-0001-9873-4018; Email: tm.kumar@dignityhealth.org

Authors

Sandhya Bansal − *Norton Thoracic Institute, St. Joseph's Hospital and Medical Center, Phoenix, Arizona 85013, United States*

Marissa McGilvrey − *Collaborative Center for Translational Mass Spectrometry (CCTMS), Translational Genomics Research Institute (TGen), Phoenix, Arizona 85004, United States*

Krystine Garcia-Mansfield − *Collaborative Center for Translational Mass Spectrometry (CCTMS), Translational Genomics Research Institute (TGen), Phoenix, Arizona 85004, United States*

Ritin Sharma − *Collaborative Center for Translational Mass Spectrometry (CCTMS), Translational Genomics Research*

Institute (TGen), Phoenix, Arizona 85004, United States; ⓞ orcid.org/0000-0001-8365-9916

Ross M. Bremner − *Norton Thoracic Institute, St. Joseph's Hospital and Medical Center, Phoenix, Arizona 85013, United States*

Michael A. Smith − *Norton Thoracic Institute, St. Joseph's Hospital and Medical Center, Phoenix, Arizona 85013, United States*

Ramsey Hachem − *Department of Medicine, Washington University School of Medicine, St. Louis, Missouri 63110, United States*

Patrick Pirrotte − *Collaborative Center for Translational Mass Spectrometry (CCTMS), Translational Genomics Research Institute (TGen), Phoenix, Arizona 85004, United States*

Complete contact information is available at:
https://pubs.acs.org/10.1021/acsomega.0c00859

Author Contributions

S.B. and M.M. contributed equally to the work. T.M. and P.P. are co-senior authors. T.M. and P.P. conceived and designed the project. S.B. performed the experiments and wrote the manuscript. M.M., K.G.-M., R.S., and P.P. conducted and analyzed the experiments and revised the manuscript. R.M.B., M.A.S., and R.H. selected the patients. All authors read and approved the final manuscript.

Notes

The authors declare no competing financial interest.
The data sets generated and analyzed during the current study are available from the corresponding author upon reasonable request.

◼ ACKNOWLEDGMENTS

◼ ABBREVIATIONS USED

Abs, antibodies; AR, acute rejection; BOS, bronchiolitis obliterans syndrome; CPN1, carboxypeptidase N catalytic chain; DSA, donor-specific antibody; EV, extracellular vesicle; FC, fold change; GSEA, gene set enrichment analysis; HLA, human leukocyte antigen; IGCL7, immunoglobulin lambda constant 7; LC−MS/MS, liquid chromatograph−mass spectrometry; LTx, lung transplant; LTxR, lung transplant recipient; MST1, macrophage-stimulating protein; PBS, phosphate-buffered saline; PIGR, polymeric immunoglobulin receptor; RAS, restrictive allograft syndrome; RVI, respiratory viral infection; SAg, self-antigen

◼ REFERENCES

(1) Aziz, F.; Penupolu, S.; Xu, X.; He, J. Lung transplant in end-staged chronic obstructive pulmonary disease (COPD) patients: a concise review. *J. Thorac. Dis.* **2010**, *2*, 111−116.

(2) Yusen, R. D.; Christie, J. D.; Edwards, L. B.; Kucheryavaya, A. Y.; Benden, C.; Dipchand, A. I.; Dobbels, F.; Kirk, R.; Lund, L. H.; Rahmel, A. O.; Stehlik, J. The Registry of the International Society for Heart and Lung Transplantation: Thirtieth Adult Lung and Heart-Lung Transplant Report–2013; focus theme: age. *J. Heart Lung Transplant* **2013**, *32*, 965−978.

(3) Arcasoy, S. M.; Kotloff, R. M. Lung Transplantation. N. Engl. J. Med. 1999, 340, 1081−1091.

(4) Billings, J. L.; Hertz, M. I.; Savik, K.; Wendt, C. H. Respiratory viruses and chronic rejection in lung transplant recipients. J. Heart Lung Transplant. 2002, 21, 559−566.

(5) Jakubec, P.; Žurkova, M.; Hajdová, L.; Křenková, A.; Kolek, V. The complications after lung transplantation. Vnitr. Lek. 2018, 63, 848−859.

(6) Kennel, P. J.; Saha, A.; Maldonado, D. A.; Givens, R.; Brunjes, D. L.; Castillero, E.; Zhang, X.; Ji, R.; Yahi, A.; George, I.; Mancini, D. M.; Koller, A.; Fine, B.; Zorn, E.; Colombo, P. C.; Tatonetti, N.; Chen, E. I.; Schulze, P. C. Serum exosomal protein profiling for the non-invasive detection of cardiac allograft rejection. J. Heart Lung Transplant. 2018, 37, 409−417.

(7) Shah, R.; Patel, T.; Freedman, J. E. Circulating Extracellular Vesicles in Human Disease. N. Engl. J. Med. 2018, 379, 958−966.

(8) Valadi, H.; Ekström, K.; Bossios, A.; Sjöstrand, M.; Lee, J. J.; Lötvall, J. O. Exosome-mediated transfer of mRNAs and microRNAs is a novel mechanism of genetic exchange between cells. Nat. Cell Biol. 2007, 9, 654−659.

(9) De Toro, J.; Herschlik, L.; Waldner, C.; Mongini, C. Emerging roles of exosomes in normal and pathological conditions: new insights for diagnosis and therapeutic applications. Front. Immunol. 2015, 6, No. 203.

(10) Gunasekaran, M.; Sharma, M.; Hachem, R.; Bremner, R.; Smith, M. A.; Mohanakumar, T. Circulating Exosomes with Distinct Properties during Chronic Lung Allograft Rejection. J. Immunol. 2018, 200, 2535−2541.

(11) Sharma, M.; Ravichandran, R.; Bansal, S.; Bremner, R. M.; Smith, M. A.; Mohanakumar, T. Tissue-associated self-antigens containing exosomes: Role in allograft rejection. Hum. Immunol. 2018, 79, 653−658.

(12) Naesens, M.; Li, L.; Ying, L.; Sansanwal, P.; Sigdel, T. K.; Hsieh, S. C.; Kambham, N.; Lerut, E.; Salvatierra, O.; Butte, A. J.; Sarwal, M. M. Expression of complement components differs between kidney allografts from living and deceased donors. J. Am. Soc. Nephrol. 2009, 20, 1839−1851.

(13) Sis, B.; Jhangri, G. S.; Bunnag, S.; Allanach, K.; Kaplan, B.; Halloran, P. F. Endothelial gene expression in kidney transplants with alloantibody indicates antibody-mediated damage despite lack of C4d staining. Am. J. Transplant. 2009, 9, 2312−2323.

(14) Skidgel, R. A. Structure and Function of Mammalian Zinc Carboxypeptidase. In Zinc Metalloproteases In Health and Disease; Taylor & Francis: London, 1996.

(15) Kaetzel, C. S.; Robinson, J. K.; Chintalacharuvu, K. R.; Vaerman, J. P.; Lamm, M. E. The polymeric immunoglobulin receptor (secretory component) mediates transport of immune complexes across epithelial cells: a local defense function for IgA. Proc. Natl. Acad. Sci. U.S.A. 1991, 88, 8796−8800.

(16) Patti, M. G.; Vela, M. F.; Odell, D. D.; Richter, J. E.; Fisichella, P. M.; Vaezi, M. F. The Intersection of GERD, Aspiration, and Lung Transplantation. J. Laparoendosc. Adv. Surg. Tech. A 2016, 26, 501−505.

(17) Bezerra, J. A.; Han, S.; Danton, M. J. S.; Degen, S. J. Are hepatocyte growth factor-like protein and macrophage stimulating protein the same protein? Protein Sci. 1193, 2, 666−668.

(18) Wilson, C. B.; Ray, M.; Lutz, M.; Sharda, D.; Xu, J.; Hankey, P. A. The RON receptor tyrosine kinase regulates IFN-gamma production and responses in innate immunity. J. Immunol. 2008, 181, 2303−2310.

(19) Narasaraju, T.; Yang, E.; Samy, R. P.; Tan, K. S.; Moorthy, A. N.; Phoon, M. C.; van Rooijen, N.; Choi, H. W.; Chow, V. T. Combination therapy with hepatocyte growth factor and oseltamivir confers enhanced protection against influenza viral pneumonia. Curr. Mol. Med. 2014, 14, 690−702.

(20) Sundaresan, S.; Mohanakumar, T.; Smith, M. A.; Trulock, E. P.; Lynch, J.; Phelan, D.; Cooper, J. D.; Patterson, G. A. HLA-A locus mismatches and development of antibodies to HLA after lung transplantation correlate with the development of bronchiolitis obliterans syndrome. Transplantation 1998, 65, 648−653.

(21) Hachem, R. R.; Tiriveedhi, V.; Patterson, G. A.; Aloush, A.; Trulock, E. P.; Mohanakumar, T. Antibodies to K-alpha 1 tubulin and collagen V are associated with chronic rejection after lung transplantation. Am. J. Transplant. 2012, 12, 2164−2171.

(22) Bharat, A.; Saini, D.; Steward, N.; Hachem, R.; Trulock, E. P.; Patterson, G. A.; Meyers, B. F.; Mohanakumar, T. Antibodies to self-antigens predispose to primary lung allograft dysfunction and chronic rejection. Ann. Thorac. Surg. 2010, 90, 1094−1101.

(23) Saini, D.; Weber, J.; Ramachandran, S.; Phelan, D.; Tiriveedhi, V.; Liu, M.; Steward, N.; Aloush, A.; Hachem, R.; Trulock, E.; Meyers, B.; Patterson, G. A.; Mohanakumar, T. Alloimmunity-induced autoimmunity as a potential mechanism in the pathogenesis of chronic rejection of human lung allografts. J. Heart Lung Transplant. 2011, 30, 624−631.

(24) Meyer, K. C.; Raghu, G.; Verleden, G. M.; Corris, P. A.; Aurora, P.; Wilson, K. C.; Brozek, J.; Glanville, A. R. An international ISHLT/ ATS/ERS clinical practice guideline: diagnosis and management of bronchiolitis obliterans syndrome. Eur. Respir. J. 2014, 44, 1479−1503.

(25) Gunasekaran, M.; Xu, Z.; Nayak, D. K.; Sharma, M.; Hachem, R.; Walia, R.; Bremner, R. M.; Smith, M. A.; Mohanakumar, T. Donor-Derived Exosomes With Lung Self-Antigens in Human Lung Allograft Rejection. Am. J. Transplant. 2017, 17, 474−484.

(26) Théry, C.; Witwer, K. W.; Aikawa, E.; Alcaraz, M. J.; Anderson, J. D.; Andriantsitohaina, R.; Antoniou, A.; Arab, T.; Archer, F.; Atkin-Smith, G. K.; Ayre, D. C.; Bach, J. M.; Bachurski, D.; Baharvand, H.; Balaj, L.; Baldacchino, S.; Bauer, N. N.; Baxter, A. A.; Bebawy, M.; Beckham, C.; Bedina Zavec, A.; Benmoussa, A.; Berardi, A. C.; Bergese, P.; Bielska, E.; Blenkiron, C.; Bobis-Wozowicz, S.; Boilard, E.; Boireau, W.; Bongiovanni, A.; Borras, F. E.; Bosch, S.; Boulanger, C. M.; Breakefield, X.; Breglio, A. M.; Brennan, M. A.; Brigstock, D. R.; Brisson, A.; Broekman, M. L.; Bromberg, J. F.; Bryl-Gorecka, P.; Buch, S.; Buck, A. H.; Burger, D.; Busatto, S.; Buschmann, D.; Bussolati, B.; Buzas, E. I.; Byrd, J. B.; Camussi, G.; Carter, D. R.; Caruso, S.; Chamley, L. W.; Chang, Y. T.; Chen, C.; Chen, S.; Cheng, L.; Chin, A. R.; Clayton, A.; Clerici, S. P.; Cocks, A.; Cocucci, E.; Coffey, R. J.; Cordeiro-da-Silva, A.; Couch, Y.; Coumans, F. A.; Coyle, B.; Crescitelli, R.; Criado, M. F.; D'Souza-Schorey, C.; Das, S.; Datta Chaudhuri, A.; de Candia, P.; De Santana, E. F.; De Wever, O.; Del Portillo, H. A.; Demaret, T.; Deville, S.; Devitt, A.; Dhondt, B.; Di Vizio, D.; Dieterich, L. C.; Dolo, V.; Dominguez Rubio, A. P.; Dominici, M.; Dourado, M. R.; Driedonks, T. A.; Duarte, F. V.; Duncan, H. M.; Eichenberger, R. M.; Ekstrom, K.; El Andaloussi, S.; Elie-Caille, C.; Erdbrugger, U.; Falcon-Perez, J. M.; Fatima, F.; Fish, J. E.; Flores-Bellver, M.; Forsonits, A.; Frelet-Barrand, A.; Fricke, F.; Fuhrmann, G.; Gabrielsson, S.; Gamez-Valero, A.; Gardiner, C.; Gartner, K.; Gaudin, R.; Gho, Y. S.; Giebel, B.; Gilbert, C.; Gimona, M.; Giusti, I.; Goberdhan, D. C.; Gorgens, A.; Gorski, S. M.; Greening, D. W.; Gross, J. C.; Gualerzi, A.; Gupta, G. N.; Gustafson, D.; Handberg, A.; Haraszti, R. A.; Harrison, P.; Hegyesi, H.; Hendrix, A.; Hill, A. F.; Hochberg, F. H.; Hoffmann, K. F.; Holder, B.; Holthofer, H.; Hosseinkhani, B.; Hu, G.; Huang, Y.; Huber, V.; Hunt, S.; Ibrahim, A. G.; Ikezu, T.; Inal, J. M.; Isin, M.; Ivanova, A.; Jackson, H. K.; Jacobsen, S.; Jay, S. M.; Jayachandran, M.; Jenster, G.; Jiang, L.; Johnson, S. M.; Jones, J. C.; Jong, A.; Jovanovic-Talisman, T.; Jung, S.; Kalluri, R.; Kano, S. I.; Kaur, S.; Kawamura, Y.; Keller, E. T.; Khamari, D.; Khomyakova, E.; Khvorova, A.; Kierulf, P.; Kim, K. P.; Kislinger, T.; Klingeborn, M.; Klinke, D. J., 2nd; Kornek, M.; Kosanovic, M. M.; Kovacs, A. F.; Kramer-Albers, E. M.; Krasemann, S.; Krause, M.; Kurochkin, I. V.; Kusuma, G. D.; Kuypers, S.; Laitinen, S.; Langevin, S. M.; Languino, L. R.; Lannigan, J.; Lasser, C.; Laurent, L. C.; Lavieu, G.; Lazaro-Ibanez, E.; Le Lay, S.; Lee, M. S.; Lee, Y. X. F.; Lemos, D. S.; Lenassi, M.; Leszczynska, A.; Li, I. T.; Liao, K.; Libregts, S. F.; Ligeti, E.; Lim, R.; Lim, S. K.; Line, A.; Linnemannstons, K.; Llorente, A.; Lombard, C. A.; Lorenowicz, M. J.; Lorincz, A. M.; Lotvall, J.; Lovett, J.; Lowry, M. C.; Loyer, X.; Lu, Q.; Lukomska, B.; Lunavat, T. R.; Maas, S. L.; Malhi, H.; Marcilla, A.; Mariani, J.; Mariscal, J.;

Martens-Uzunova, E. S.; Martin-Jaular, L.; Martinez, M. C.; Martins, V. R.; Mathieu, M.; Mathivanan, S.; Maugeri, M.; McGinnis, L. K.; McVey, M. J.; Meckes, D. G., Jr.; Meehan, K. L.; Mertens, I.; Minciacchi, V. R.; Moller, A.; Moller Jorgensen, M.; Morales-Kastresana, A.; Morhayim, J.; Mullier, F.; Muraca, M.; Musante, L.; Mussack, V.; Muth, D. C.; Myburgh, K. H.; Najrana, T.; Nawaz, M.; Nazarenko, I.; Nejsum, P.; Neri, C.; Neri, T.; Nieuwland, R.; Nimrichter, L.; Nolan, J. P.; Nolte-'t Hoen, E. N.; Noren Hooten, N.; O'Driscoll, L.; O'Grady, T.; O'Loghlen, A.; Ochiya, T.; Olivier, M.; Ortiz, A.; Ortiz, L. A.; Osteikoetxea, X.; Ostergaard, O.; Ostrowski, M.; Park, J.; Pegtel, D. M.; Peinado, H.; Perut, F.; Pfaffl, M. W.; Phinney, D. G.; Pieters, B. C.; Pink, R. C.; Pisetsky, D. S.; Pogge von Strandmann, E.; Polakovicova, I.; Poon, I. K.; Powell, B. H.; Prada, I.; Pulliam, L.; Quesenberry, P.; Radeghieri, A.; Raffai, R. L.; Raimondo, S.; Rak, J.; Ramirez, M. I.; Raposo, G.; Rayyan, M. S.; Regev-Rudzki, N.; Ricklefs, F. L.; Robbins, P. D.; Roberts, D. D.; Rodrigues, S. C.; Rohde, E.; Rome, S.; Rouschop, K. M.; Rughetti, A.; Russell, A. E.; Saa, P.; Sahoo, S.; Salas-Huenuleo, E.; Sanchez, C.; Saugstad, J. A.; Saul, M. J.; Schiffelers, R. M.; Schneider, R.; Schoyen, T. H.; Scott, A.; Shahaj, E.; Sharma, S.; Shatnyeva, O.; Shekari, F.; Shelke, G. V.; Shetty, A. K.; Shiba, K.; Siljander, P. R.; Silva, A. M.; Skowronek, A.; Snyder, O. L., 2nd; Soares, R. P.; Sodar, B. W.; Soekmadji, C.; Sotillo, J.; Stahl, P. D.; Stoorvogel, W.; Stott, S. L.; Strasser, E. F.; Swift, S.; Tahara, H.; Tewari, M.; Timms, K.; Tiwari, S.; Tixeira, R.; Tkach, M.; Toh, W. S.; Tomasini, R.; Torrecilhas, A. C.; Tosar, J. P.; Toxavidis, V.; Urbanelli, L.; Vader, P.; van Balkom, B. W.; van der Grein, S. G.; Van Deun, J.; van Herwijnen, M. J.; Van Keuren-Jensen, K.; van Niel, G.; van Royen, M. E.; van Wijnen, A. J.; Vasconcelos, M. H.; Vechetti, I. J., Jr.; Veit, T. D.; Vella, L. J.; Velot, E.; Verweij, F. J.; Vestad, B.; Vinas, J. L.; Visnovitz, T.; Vukman, K. V.; Wahlgren, J.; Watson, D. C.; Wauben, M. H.; Weaver, A.; Webber, J. P.; Weber, V.; Wehman, A. M.; Weiss, D. J.; Welsh, J. A.; Wendt, S.; Wheelock, A. M.; Wiener, Z.; Witte, L.; Wolfram, J.; Xagorari, A.; Xander, P.; Xu, J.; Yan, X.; Yanez-Mo, M.; Yin, H.; Yuana, Y.; Zappulli, V.; Zarubova, J.; Zekas, V.; Zhang, J. Y.; Zhao, Z.; Zheng, L.; Zheutlin, A. R.; Zickler, A. M.; Zimmermann, P.; Zivkovic, A. M.; Zocco, D.; Zuba-Surma, E. K. Minimal information for studies of extracellular vesicles 2018 (MISEV2018): a position statement of the International Society for Extracellular Vesicles and update of the MISEV2014 guidelines. *J. Extracell. Vesicles* **2018**, *7*, No. 1535750.

(27) Manza, L. L.; Stamer, S. L.; Ham, A.-J. L.; Codreanu, S. G.; Liebler, D. C. Sample preparation and digestion for proteomic analyses using spin filters. *Proteomics* **2005**, *5*, 1742−1745.

(28) Wiśniewski, J. R.; Zougman, A.; Nagaraj, N.; Mann, M. Universal sample preparation method for proteome analysis. *Nat. Methods* **2009**, *6*, 359−362.

(29) Cox, J.; Mann, M. MaxQuant enables high peptide identification rates, individualized p.p.b.-range mass accuracies and proteome-wide protein quantification. *Nat. Biotechnol.* **2008**, *26*, 1367−1372.

(30) Welsh, E. A.; Eschrich, S. A.; Berglund, A. E.; Fenstermacher, D. A. Iterative rank-order normalization of gene expression microarray data. *BMC Bioinf.* **2013**, *14*, No. 153.

(31) Keerthikumar, S.; Chisanga, D.; Ariyaratne, D.; Al Saffar, H.; Anand, S.; Zhao, K.; Samuel, M.; Pathan, M.; Jois, M.; Chilamkurti, N.; Gangoda, L.; Mathivanan, S. ExoCarta: A Web-Based Compendium of Exosomal Cargo. *J. Mol. Biol.* **2016**, *428*, 688−692.

(32) Subramanian, A.; Tamayo, P.; Mootha, V. K.; Mukherjee, S.; Ebert, B. L.; Gillette, M. A.; Paulovich, A.; Pomeroy, S. L.; Golub, T. R.; Lander, E. S.; Mesirov, J. P. Gene set enrichment analysis: a knowledge-based approach for interpreting genome-wide expression profiles. *Proc. Natl. Acad. Sci. U.S.A.* **2005**, *102*, 15545−15550.